RSC Advances

PAPER

View Article Online
View Journal | View Issue

Cite this: RSC Adv., 2014, 4, 44614

Functional hybrids of layered double hydroxides with hemin: synergistic effect for peroxynitrite-scavenging activity

Fengmin Qiao, Weijie Shi, Jing Dong, Wei Lv* and Shiyun Ai*

Received 6th August 2014
Accepted 11th September 2014

DOI: 10.1039/c4ra08200a

www.rsc.org/advances

Hemin has been successfully modified onto the surface of CuAl layered double hydroxide nanosheets by a simple coprecipitation process, which afforded a hemin modified CuAl layered double hydroxide (H-LDH) hybrid functional material that exhibited protective effects against the harmful $ONOO^-$. The obtained products were characterized by X-ray powder diffraction, scanning electron microscopy, transmission electron microscopy and Fourier transform infrared spectroscopy, which showed that the samples had hexagonal symmetry structure with a mean lateral size of 1 μm, on the surface of which were adsorbed round particles with a diameter of about 300 nm. A detailed inhibition study on $ONOO^-$-mediated nitration reactions indicated that the interaction between hemin and LDHs results in a synergistic effect, which leads to an efficient reduction of $ONOO^-$ to nitrate. The present study suggests that the H-LDHs had an efficient $ONOO^-$ scavenging ability, and may well be a potent $ONOO^-$ scavenger for protection of the cellular defense activity against $ONOO^-$ involved diseases.

1. Introduction

Peroxynitrite ($ONOO^-$), a potent cytotoxic oxidant, is a product formed by the reaction between nitric oxide (NO) and superoxide radicals ($^{\cdot}O_2^-$).[1] Stimulated macrophages, neutrophils, endothelial cells and Kupffer cells have been known to generate $ONOO^-$.[2] $ONOO^-$ is able to induce peroxidation of lipids, oxidation of sulfhydryl group, nitration of tyrosine residue in protein,[3] and cause DNA damage.[4] Protein tyrosine residues are especially susceptible to peroxynitrite nitration.[5,6] The stable end-product, 3-nitrotyrosine, is considered to be a biomarker of peroxynitrite-specific protein damage.[7] 3-Nitrotyrosine is found in tissue specimens from several diseases, including cardiovascular disorders, degenerative neurological disorders and certain renal diseases. This suggests that peroxynitrite is involved in the pathological processes of these diseases.[8] Since endogenous scavenging enzymes responsible for $ONOO^-$ inactivation are lacking, seeking scavengers specific to $ONOO^-$ is of considerable importance. Currently, there is an increasing interest in screening products for possible $ONOO^-$ scavengers.

To develop powerful $ONOO^-$ scavengers, many different methods have been utilized. One example is to screen naturally-occurring compounds from herbal sources, including ascorbic acid,[9] flavonoids,[10] isoflavonoids,[11] ergothioneine[12,13] and polyhydroxyphenols from fruits, wine, tea, and green vegetables. While another method is to synthesize $ONOO^-$ scavengers in test tubes such as selenomethionine, selenocystine, and ebselen.[14,15]

Increasing attention has been paid to layered double hydroxides (LDHs), also known as hydrotalcite-like compounds and anionic clays. They can be represented by a general formula of $[M^{2+}_{1-x}M^{3+}x(OH)_2]^{x+}[A^{n-}_{x/n}]^{x-}\cdot mH_2O$ (M^{2+}/M^{3+}: divalent and trivalent metal cations; $x = 0.2$–0.33), which consist of octahedral brucite-like host layers, charge-balancing anions (A^{n-}), and interlayer water molecules.[16] This highly tunable intralayer composition, coupled with a wide possible choice of anionic moieties, affords large varieties of multifunctional LDH materials for potential applications including anion exchangers,[17] adsorbents,[18] catalysts,[19] solid-state nanoreactors and molecular sieves,[20] polymer composites, and bioactive materials.[21] Furthermore, the bio-compatibility and low toxicity of LDHs as green materials enables their ecological, biological and medicinal applications. Recent reports demonstrate that LDH crystals can be artificially exfoliated into macromolecular nanosheets through soft chemical procedures.[22–24] In addition, through static adsorption, functional molecules could be modified on the surface of the hydrotalcite piece.[25,26] The nanosheets are also expected to be used as building blocks for the construction of various functional nanocomposites or nanostructures.

Functionalization of LDH crystals with polar molecules imparts the hydrophilicity effects, and thus enhances its dispersibility in polar solvents.[27] Particularly, noncovalent functionalization of LDH crystals with biomolecules make the LDH crystals highly biocompatible with the conservation of intrinsic properties of LDH crystals.[28] Hemin, a well-known protoporphyrin found at the active sites of hemin proteins, plays a key

College of Chemistry and Material Science, Shandong Agricultural University, Taian, 271018, P. R. China. E-mail: ashy@sdau.edu.cn; Fax: +86 538 8242251; Tel: +86 538 8247660

role in biochemical reactions and electron-transport chain.[29,30] Accordingly, hemin was stabilized on LDHs sheets by non-covalent functionalization through π–π interactions to yield hemin-functionalized CuAl-layered double hydroxides (H-LDHs) hybrid microchips. Herein, we describe a coprecipitation method for the construction of H-LDHs microchips. We also demonstrate, to our knowledge, for the first time, that H-LDHs microchips exhibit remarkable peroxynitrite-scavenging activities. The data support the conclusion that H-LDHs can exhibit a biological function by acting as a peroxynitrite scavenger. Scavenging activity has a wide range of practical applications. From the chemical and medicinal point of view, the ability to catalyse isomerization and reduction of $ONOO^-$ and scavenging of $^{\bullet}NO_2$ to reduce their toxicity is frequently used in the pathological processes of related disease.

2. Experimental section

2.1 Reagents and apparatus

Copper nitrate ($Cu(NO_3)_2 \cdot 3H_2O$), Aluminium nitrate ($Al(NO_3)_2 \cdot 9H_2O$) were purchased from Aladdin (Shanghai, China). Sodium hydroxide (NaOH), absolute ethyl alcohol (CH_3CH_2OH), hydrogen peroxide (H_2O_2), sodium nitrite ($NaNO_2$), ammonium hydroxide ($NH_3 \cdot H_2O$), sodium hydrogen carbonate ($NaHCO_3$) were purchased from Kay Tong Chemical Reagents Co. Ltd (Tianjin, China). L-tyrosine($C_3H_{11}NO_3$) and hemin($C_{34}H_{32}ClFeN_4O_4$) were purchased from Shanghai Bio Science & Technology Co. Ltd (Shanghai, China). Phosphatic buffer solution (100 mM, pH value range from 5.5 to 11.5) were used in this work and double distilled deionized water was applied throughout the experiment. All chemicals used in this work were of analytical grade and used as received without further purification.

2.2 Preparation of hemin-functionalized CuAl-layered double hydroxides

Hemin-functionalized CuAl-layered double hydroxides (H-LDHs) with different content of hemin were prepared by the coprecipitation method adapted for enzyme solution.[31] Typically, hemin (1 mg) was firstly dissolved in 20 mL ethanol by the addition of 80 μL NH_3 to get dark reddish-brown solution. A mixed aqueous solution of $Cu(NO_3)_2$ and $Al(NO_3)_3$, with a Cu^{2+}/Al^{3+} molar ratio $r = 2$ and a total concentration of metallic cations of 100 mM, was introduced into the above dark reddish-brown solution. The pH was maintained constant at a value of 9.0 during all the coprecipitation by the simultaneous addition of a 2 M NaOH solution. This solution was purged by a nitrogen gas flow to expel air/O_2. After aged at room temperature with stirring for 6 h, the sample was filtered, washed with water, and air-dried for physical characterization. Samples with different content of hemin (5, 10, 15, 20, 25, 30 mg) were prepared by the same method. For the sake of convenience in writing, H-LDHs with different contents of hemin (1, 5, 10, 15, 20, 25, 30 mg) were aliased as H-LDH (1), H-LDH (2), H-LDH (3), H-LDH (4), H-LDH (5), H-LDH (6), H-LDH (7), respectively. For comparison, native LDH was prepared by the same method without introducing hemin solution.

The morphology and size distribution of the product were studied by using a JEM-2010 transmission electron microscope (TEM, Japan) and a JSM-6610 scanning electron microscopy (SEM, Japan).The crystal phase was investigated by a Rigaku DLMAX-2550 V diffractometer (40 kV, Cu Kα ($\lambda = 1.54056$ Å), 2θ range 5–80°; scan speed of 6° per min). Fourier transform infrared (FT-IR) spectra were obtained on a Thermo Nicolet-380 IR spectrophotometer (USA).

2.3 Preparation of peroxynitrite

Peroxynitrite (PN) was prepared using a quenched-flow reactor as described in the literature.[32] A 20.00 mL solution containing 0.6 M HCl and 0.7 M H_2O_2 was rapidly mixed with an equal volume of solution containing 0.6 M $NaNO_2$ in ice-water bath, the above reaction was quenched by 1.5 M NaOH with volume of 30.00 mL simultaneously. The excess H_2O_2 was eliminated by a small amount of MnO_2 powder. The resulting solution was filtered and obtained light yellow filtrate, which could be stably stored at −20 °C for several weeks. The concentration (2.41 mM) of the peroxynitrite stock solution was determined by measuring the absorbance at 302 nm using a molar extinction coefficient of 1670 M^{-1} cm^{-1} at 302 nm using a UV-2450 Shimadzu Vis-spectrometer.[33]

2.4 Reaction of tyrosine with peroxynitrite

The reaction between tyrosine and $ONOO^-$ was investigated. 400 μL increasing final concentration of $ONOO^-$ (from 0.08 mM to 2.41 mM) was reacted with 400 μL tyrosine (0.86 mM) in pre-blended solution containing 400 μL phosphate buffer (100 mM, pH 7.5) and 200 μL Sodium hydrogen carbonate ($NaHCO_3$, 0.14 M) at room temperature for 10 min, followed by a spectrophotometric scan with a UV-2450 Shimadzu Vis-spectrometer from 300 to 600 nm.

To test the influence of temperature and pH on tyrosine nitration, peroxynitrite (2.41 mM) was added to 0.86 mM tyrosine in phosphate buffer (100 mM) at a range of temperatures (0–55 °C) or a range of values of pH (5.5–11.5) for 10 min incubation, the absorbance at 426 nm was determined.

2.5 Investigation of the peroxynitrite-scavenging activities of H-LDHs

The peroxynitrite-scavenging activity of the H-LDHs (hemin content 20 mg) was evaluated on the basis of the decomposition of peroxynitrite. The scavenger was added into $ONOO^-$ stock solution, the reaction process of equivalent H-LDHs, LDHs and hemin with 400 μL $ONOO^-$ were monitored in timescan mode at 302 nm using a UV-2450 Shimadzu Vis-spectrometer.

2.6 Inhibition of peroxynitrite-mediated tyrosine nitration by H-LDHs

The peroxynitrite-scavenging activity of the H-LDHs was evaluated based on the inhibition of peroxynitrite-induced nitration of free tyrosine. The nitration of tyrosine was performed as

previously reported. Briefly, We employed a mixture containing L-tyrosine (0.86 mM), sodium hydrogen carbonate ($NaHCO_3$, 0.14 M) and $ONOO^-$ (2.41 mM) in sodium phosphate buffer (100 mM, pH 7.5) without and with increasing content of hemin in H-LDHs at 35 °C. It was incubated for 10 min before recording absorbance. The formation of 3-nitrotyrosine was monitored at the wavelength 426 nm using UV/vis spectroscopy.

2.7 Investigation of the H-LDHs's cyclic utilization

In order to explore whether the product H-LDHs can be reused for the scavenging of peroxynitrite, the same test was repeated for five times. Briefly, the inhibition of peroxynitrite-mediated tyrosine nitration by H-LDHs (1.2 mg) was performed as previously reported. Soon afterwards, the reaction solution still containing H-LDHs was centrifuged and washed several times with decarbonated water, and finally dried in air at room temperature for the next use. In each time, the formation of 3-nitrotyrosine was monitored at the wavelength 426 nm using UV/vis spectroscopy to test the H-LDHs' inhibition performance.

2.8 PN scavenging activity in PN-mediated protein (BSA) nitration

In terms of bovine serum albumin (BSA), the nitration was performed by the addition of PN (2.41 mM) to BSA (0.29 mM) in 100 mM phosphate buffer of pH 7.5 at 35 °C. The reaction mixture was incubated for 10 min. Similarly, the reactions of BSA with PN were performed in the absence and presence of H-LDHs. The formation of 3-nitrotyrosine was monitored at the wavelength 426 nm using UV/vis spectroscopy.

3. Results and discussions

3.1 Characterization of the H-LDHs

The non-covalently grafted hemin on LDHs was characterized by various methods. Fig. 1a shows TEM images of H-LDHs sample. As can be seen, the sample consisted of irregular and thin hexagonal platelets with a mean lateral size as large as 1 μm and a thickness of about 30 nm. In addition, on the surface of LDHs, round particles with a diameter of about 300 nm, are also observed. The TEM (Fig. 1a) and SEM images (Fig. 1b) of H-LDHs hybrid showed flaky features with folded morphologies and round particles absorbed on surface. As is known, the native LDHs displays uniform and thin hexagonal platelets, whereas the presence of biomolecules in the reactive medium leads to quite different sample morphology.[34–36] It seems that the modification of the LDHs surface by the covering of hemin induces such aggregation of platelets strongly associated with the biomolecules. As determined by EDS (Fig. 1c), the predominant elements in the H-LDHs samples were Cu, Al and O in various compounds. Lesser amounts of the elements Fe, N and C were also observed.

As shown in Fig. 2, the interactions between hemin and CuAl LDHs were investigated by FT-IR. Spectrum a shows a sharp band at 3408 cm^{-1}, attributed to the OH stretching mode, which is characteristic of free OH groups in brucite-like

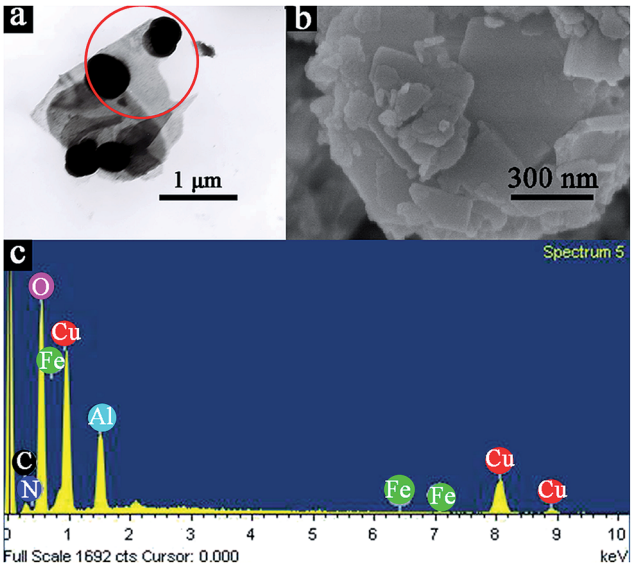

Fig. 1 (a) TEM; (b) SEM; (c) EDS images of hemin modified CuAl-LDHs nanocomposite.

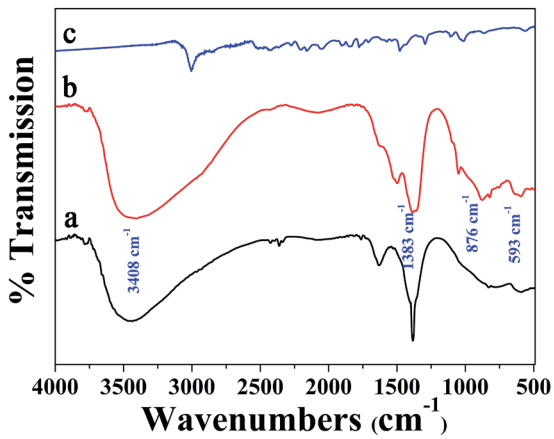

Fig. 2 FT-IR spectra of (a) CuAl LDHs, (b) heme modified H-LDHs, (c) heme.

structures. A broad absorption in the low-frequency region (593 and 876 cm^{-1}) may be assigned to M–O (M:Cu/Al) stretching and M–OH bending vibrations in the octahedral hydroxyl sheets. After treatment with hemin (spectrum b), a broad band centered at 3408 cm^{-1} replaces the sharp band of the OH stretching mode, which is usually interpreted as stretching modes of OH groups with hydrogen bonding and of interlayer hemin molecules. In particular, the bands at 876, 593 cm^{-1} sharpens strongly and the bands at 1386 cm^{-1} are markedly enlarged. Obviously, these changes are due to the formation of hydrogen bonding, π–π interaction between LDHs sheets and hemin. For the loading of hemin, the broadening and enlarging of nitrate can be explained by the coverage of the LDH surface by hemin, while when the surface is not saturated by the hemin, the NO_3^{2-} anions ensure the charge compensation of the lattice. The vibration bands of the confined heme are at the

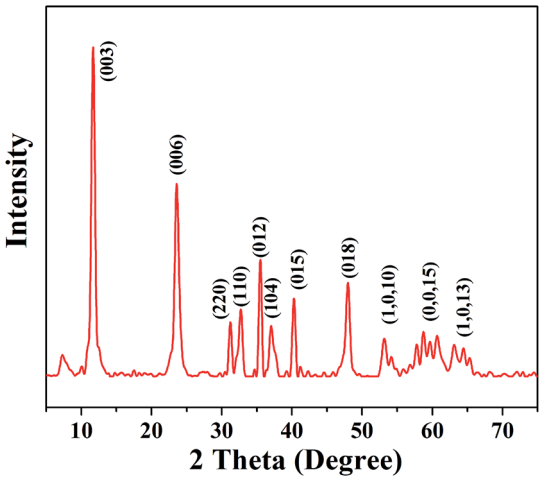

Fig. 3 XRD spectra of heme modified H-LDHs.

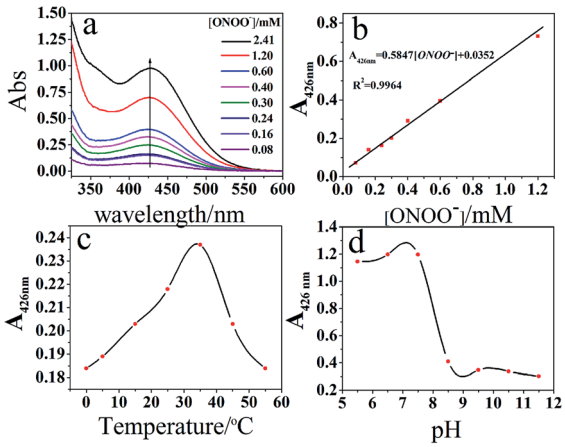

Fig. 4 a) Nitration of free L-tyrosine with increasing concentration of peroxynitrite and (b) linear fitting. Dependency of the PN-mediated nitration of free L-tyrosine on Temperature (c) and pH (d). Experiments were carried out using 2.41 mM $ONOO^-$ in 400 μL sodium phosphate buffer (100 mM) contains 0.86 mM L-tyrosine, 0.14 M sodium hydrogen carbonate.

same wavelength position than those of the free enzyme, suggesting that the molecular structure of the heme seems to be preserved after being absorbed onto the inorganic materials.

Fig. 3 showed the X-ray powder diffraction (XRD) pattern of H-LDHs composites, and the XRD pattern showed that they have a hexagonal symmetry, the same as reported in the literature.[37] The characteristic diffraction peaks of H-LDHs still appeared after interaction, revealing that the process of hemin adsorption did not do damage to the interlayer structure of LDHs. They all had a good crystallinity. The new peaks appeared might be caused by the coordinate bond which formed after hemin was adsorbed on the surface of LDHs. Obviously, the presence of the (012) and (110) diffraction lines evidence the formation of the layered structure. The basal spacing of LDHs was around 0.7 nm before adsorption and tiny changes appeared on it after adsorption.[37] The changes of the basal spacing on LDHs before and after adsorption may due to the loss of H_2O molecules inside or on the surface of LDHs. It can be concluded that hemin was not intercalated into the interlayer of LDHs but just was adsorbed on the surface of them.

3.2 The reaction of tyrosine with PN and conditions optimization

Tyrosine undergoes the nitration process to form 3-nitrotyrosine when it is exposed to $ONOO^-$ at pH 7, showing a peak at 426 nm. In the present study, it was found that exposure of tyrosine (0.86 mM) to increasing concentrations of $ONOO^-$ (8–241 μM) resulted in an increased production of 3-nitrotyrosine (Fig. 4a) with a linear dependence in the linear range of $ONOO^-$ from 8 to 120 μM. Nitration of tyrosine can be easily detected by color change from colorless to the characteristic yellow color when tyrosine and $ONOO^-$ are mixed.

The temperature dependence of the conversion yield of tyrosine into 3-nitrotyrosine with peroxynitrite was studied in the range of 0–55 °C. The yield of 3-nitrotyrosine offers upgrading firstly and descending latter tendency with the maximal absorbance at 35 °C, which is approximately equal to the normal temperature of human body (Fig. 4c). Fig. 4d showed the impact of pH on the tyrosine nitration. As shown, under acid conditions, the content of 3-nitrotyrosine in the reaction products is less. Once nitrotyrosine was formed at pH 7.5, the absorbance was maximal at the 426 nm. Then, with the increasing pH of solution, the content of 3-nitrotyrosine decreased dramatically. $ONOO^-$ could stay stable under alkaline conditions, while the content of 3-nitrotyrosine decreased, this phenomenon implies that tyrosine nitration is not the result of direct reaction between tyrosine and $ONOO^-$. By contrast, under acid and neutral conditions, $ONOO^-$ was protonated into ONOOH, therefore reaction between tyrosine and ONOOH could induce nitration of tyrosine.

3.3 Investigation of the peroxynitrite-scavenging activities of H-LDHs

To determine the mechanism of $ONOO^-$ scavenging activity for H-LDHs, the reaction process of scavengers with $ONOO^-$ was investigated. The spectrum changes at 426 nm were monitored spectrophotometrically to ascertain whether H-LDHs undergoes a scavenging nitration process when reacting with $ONOO^-$ (8.42 mM). As shown in Fig. 5, compared with system (a) in which the peroxynitrite exists on its own at the start, the absorbance of $ONOO^-$ in system (b), (c) and (d) decreased in turn. Obviously, the decomposition rate of peroxynitrite of system (d) in which the peroxynitrite was mixed with H-LDHs is far faster than that of system (b) and (c), which indicates that the $ONOO^-$ scavenging activity of hemin is increased by about 10-fold upon functionalization with LDHs. Treatment of LDHs with hemin afforded a functional hemin-modified (H-LDHs) hybrid material that exhibited remarkable protective effects against the potentially harmful peroxynitrite.

These observations suggest that LDHs may act synergistically with hemin in exhibiting the $ONOO^-$ scavenging activity. This is probably due to the π donor property of LDHs to the Fe center of

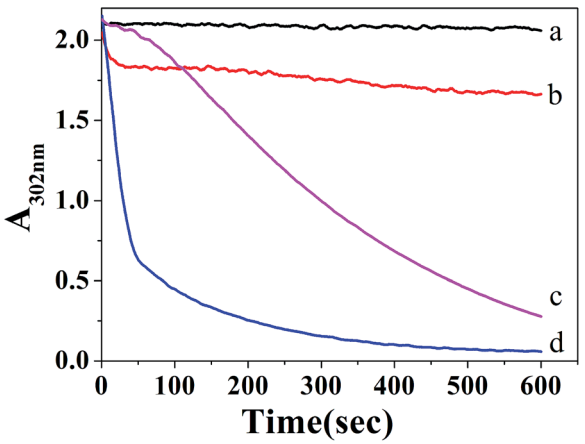

Fig. 5 Time course of peroxynitrite decomposition without (a) and with equivalent weight of LDHs (b), Heme (c),and H-LDHs (d). Peroxynitrite (8.42 mM) was mixed with scavengers at room temperature, and the reaction was followed at 302 nm.

hemin through cationic π interactions. As described for this mechanism (Scheme 1), $ONOO^-$ reacts with the Fe^{III} center in the H-LDHs to generate Fe^{III}–OONO. The homolysis of the O–O bond in Fe^{III}–OONO leads to the formation of caged radical Fe^{IV}=O·NO_2 intermediate. The LDHs layers may help to increase the local ·NO_2 and decrease their escape, which result in the recombination of Fe^{IV}=O and ·NO_2. Therefore, the reconstruction of Fe^{IV}=O and ·NO_2 generates the Fe^{III}-nitrato. The break of the Fe–O in the Fe^{III}–ONO_2 regenerates the Fe^{III} center with an elimination of nitrate (NO_3^-). The major effect of LDHs is to minimize the ·NO_2 escape reaction that is usually observed for free hemin. It should be noted that the rapid diffusion of ·NO_2 from the hemin site is the reason for the nitration of free tyrosine and tyrosine residues in protein. As reported that nitrotyrosine is formed *via* a radical reaction of tyrosine with ·OH and ·NO_2 that have escaped from a solvent-caged radical pair of ONOOH. During this reaction, Tyr-O· is first formed through the reaction of tyrosine with either ·OH or ·NO_2, and then nitrotyrosine is produced by a coupling of radicals Tyr-O· and ·NO_2.[5] These observations suggest that the π–π interactions between the LDHs and hemin play a significant role in the observed scavenging effect.

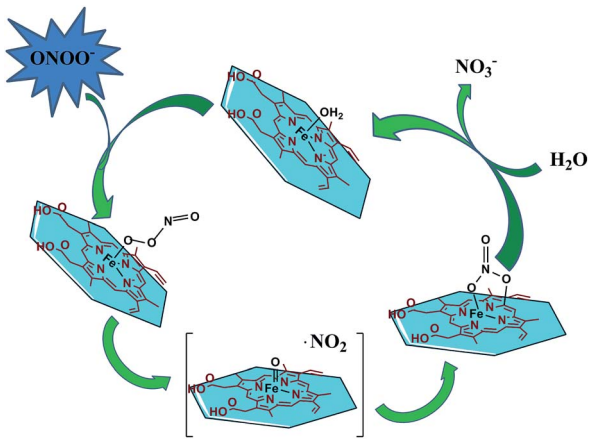

Scheme 1 Proposed mechanism for the isomerization and reduction of $ONOO^-$ and scavenging or ·NO_2 by H-LDHs hybrid nanosheets.

3.4 Inhibition of peroxynitrite-mediated tyrosine nitration by H-LDHs

In the present study, when free hemin or LDHs was tested as a scavenger of PN in PN-mediated nitration of free L-tyrosine, little scavenging activity was observed (Fig. 4). Peroxynitrite (8.42 mM) produced approximately a 50-fold increase in nitrotyrosine compared to degraded peroxynitrite (Fig. 6). Interestingly, when H-LDHs was employed as a scavenger, incubation of H-LDHs with tyrosine prior to the addition of $ONOO^-$ resulted in the decrease and even disappearance of the nitrotyrosine peak at 426 nm, implying that H-LDHs suppressed the formation of nitrotyrosine. To evaluate the potency of H-LDHs to block nitration, a full weight/weight hemin/LDHs ratio-response histogram for the inhibition of nitrotyrosine formation was generated. This histogram revealed that H-LDHs was a potent inhibitor of nitration. As is presented intuitively, the extent of this inhibition was dose-dependent. With the increasing of the content of hemin adsorbed on the LDHs surface during the coprecipitation route, the PN-scavenging capacity enhanced successively. As mentioned earlier, synergistic effect of H-LDHs plays a major role in scavenging of PN in these potentially harmful PN-mediated reactions.

3.5 Recycling properties of H-LDHs for scavenging PN

In summary, the H-LDHs has been used several times as a scavenger in PN-mediated nitration of free L-tyrosine. A simple recycling procedure has been developed and has led to the reuse of the scavenging peroxynitrite up to four times without

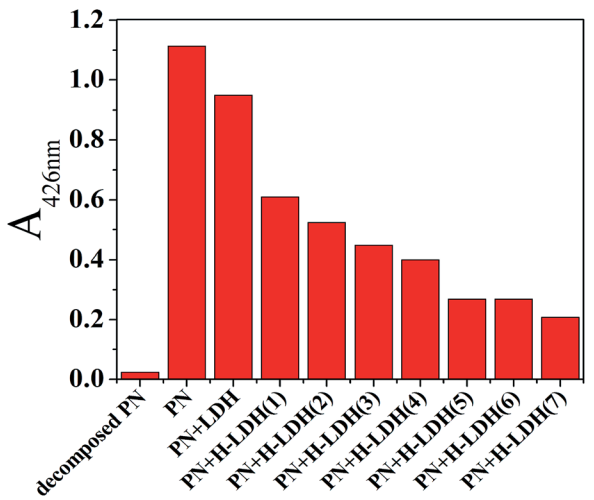

Fig. 6 PN scavenging activity in PN-mediated nitration of L-tyrosine in the presence of various concentrations of H-LDHs. Experiments were carried out in 400 μL sodium phosphate buffer (100 mM, pH 7.5) contains 0.86 mM L-tyrosine, 0.14 M Sodium hydrogen carbonate, the above solution were mixed with PN treated in the absence and presence of increasing concentration of scavengers.

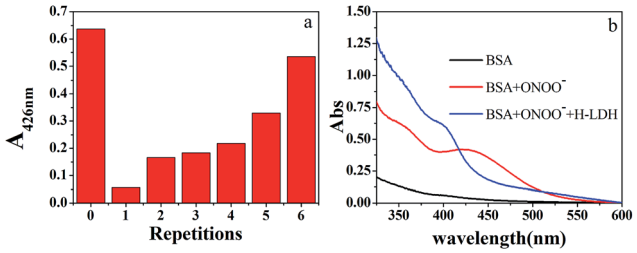

Fig. 7 (a) Recycling properties of H-LDHs for scavenging PN in PN-mediated nitration of free L-tyrosine; (b) Effect of H-LDHs with peroxynitrite-mediated nitration of BSA. BSA (1 mM) was incubated without (the red line) or with (the blue line) H-LDHs prior to the addition of $ONOO^-$. Each mixed solution was incubated at 35 °C with shaking for 10 min and scanned between 300 and 600 nm with spectrophotometric analysis. The spectrum of the peak displayed at 426 nm reflects the formation of 3-nitrotyrosine.

significant loss of activity (Fig. 7a), which were obtained in good yields and high purities. We have therefore developed a cost-effective procedure that allows recycling of the large amounts of scavenger H-LDHs required for the scavenging peroxynitrite in PN-mediated nitration of free L-tyrosine.

3.6 H-LDHs scavenging activity in PN-mediated protein (BSA) nitration

The findings that H-LDHs prevented the cytotoxicity of the peroxynitrite, suggested that H-LDHs may act as a functional peroxynitrite scavenger. Peroxynitrite modifies protein tyrosine residues through a nitration reaction to form nitrotyrosine, which is considered to be a biomarker for $ONOO^-$ oxidation. To address the scavenging activity of H-LDHs more directly, the ability of H-LDHs to block nitration of protein tyrosine residues by peroxynitrite was tested by incubating authentic peroxynitrite with BSA in the presence of H-LDHs. As shown in the Fig. 7b, nitration of BSA can be easily detected when BSA and $ONOO^-$ are mixed. Incubation of H-LDHs with BSA prior to the addition of $ONOO^-$ resulted in the disappearance of the nitrotyrosine peak at 426 nm, implying that H-LDHs inhibited the formation of 3-nitrotyrosine under the environment of protein.

4. Conclusions

In this work, a facile and efficient approach for the synthesis of hemin-functionalized CuAl-layered double hydroxides hybrid material by the coprecipitation method has been described. The internal representation showed that the obtained products were hexagonal symmetry structures, and on the surface of hexagonal platelets adsorbed round particles hemin. Noncovalent functionalization of LDHs with hemin resulted in the material that exhibits a remarkable $ONOO^-$ scavenging activity under physiologically relevant conditions. The stabilization of hemin on LDHs provides the required synergistic effect for an efficient scavenging of $ONOO^-$. In further studies, H-LDHs also showed a significant ability of inhibiting nitration of tyrosine and tyrosine residue in bovine serum albumin. The present study suggests that H-LDHs has an efficient $ONOO^-$ scavenging ability, which may well be a potent $ONOO^-$ scavenger for the protection of the cellular defense activity against the $ONOO^-$ involved diseases.

Acknowledgements

This work was supported by the National Natural Science Foundation of China (no. 21375079, 21105056) and Project of Development of Science and Technology of Shandong Province, China (no. 2013GZX20109).

Notes and references

1 J. S. Beckman and W. H. Koppenol, *Am. J. Physiol.: Cell Physiol.*, 1996, **271**, C1424–C1437.
2 S. Padmaja and R. Huie, *Biochem. Biophys. Res. Commun.*, 1993, **195**, 539–544.
3 V. Darley-Usmar and B. Halliwell, *Pharm. Res.*, 1996, **13**, 649–662.
4 J. P. Spencer, J. Wong, A. Jenner, O. I. Aruoma, C. E. Cross and B. Halliwell, *Chem. Res. Toxicol.*, 1996, **9**, 1152–1158.
5 T. Sawa, T. Akaike and H. Maeda, *J. Biol. Chem.*, 2000, **275**, 32467–32474.
6 C. D. Reiter, R.-J. Teng and J. S. Beckman, *J. Biol. Chem.*, 2000, **275**, 32460–32466.
7 L. Virág, É. Szabó, P. Gergely and C. Szabó, *Toxicol. Lett.*, 2003, **140**, 113–124.
8 H. Ischiropoulos and J. S. Beckman, *J. Clin. Invest.*, 2003, **111**, 163–169.
9 M. Sandoval, X.-J. Zhang, X. Liu, E. E. Mannick, D. A. Clark and M. J. Miller, *Free Radical Biol. Med.*, 1997, **22**, 489–495.
10 G. R. Haenen, J. B. Paquay, R. E. Korthouwer and A. Bast, *Biochem. Biophys. Res. Commun.*, 1997, **236**, 591–593.
11 B. J. Boersma, R. P. Patel, M. Kirk, P. L. Jackson, D. Muccio, V. M. Darley-Usmar and S. Barnes, *Arch. Biochem. Biophys.*, 1999, **368**, 265–275.
12 P. E. Hartman, *Methods Enzymol.*, 1990, **186**, 310–318.
13 O. I. Aruoma, M. Whiteman, T. G. England and B. Halliwell, *Biochem. Biophys. Res. Commun.*, 1997, **231**, 389–391.
14 H. Sies and H. Masumoto, *Adv. Pharmacol.*, 1996, **38**, 229–246.
15 X. Zhang, S. Mansouri, D. Mbeh, L. H. Yahia, E. Sacher and T. Veres, *Langmuir*, 2012, **28**, 12879–12885.
16 Z. P. Xu, P. S. Braterman, K. Yu, H. Xu, Y. Wang and C. J. Brinker, *Chem. Mater.*, 2004, **16**, 2750–2756.
17 M. Ulibarri, I. Pavlovic, C. Barriga, M. Hermosın and J. Cornejo, *Appl. Clay Sci.*, 2001, **18**, 17–27.
18 P. C. Pavan, E. L. Crepaldi and J. B. Valim, *J. Colloid Interface Sci.*, 2000, **229**, 346–352.
19 F. Li, Q. Tan, D. G. Evans and X. Duan, *Catal. Lett.*, 2005, **99**, 151–156.
20 C. Gérardin, D. Kostadinova, N. Sanson, B. Coq and D. Tichit, *Chem. Mater.*, 2005, **17**, 6473–6478.
21 M. Darder, M. López-Blanco, P. Aranda, F. Leroux and E. Ruiz-Hitzky, *Chem. Mater.*, 2005, **17**, 1969–1977.
22 M. Adachi-Pagano, C. Forano and J.-P. Besse, *Chem. Commun.*, 2000, 91–92.

23 R. Ma, Z. Liu, L. Li, N. Iyi and T. Sasaki, *J. Mater. Chem.*, 2006, **16**, 3809–3813.
24 Z. Liu, R. Ma, Y. Ebina, N. Iyi, K. Takada and T. Sasaki, *Langmuir*, 2007, **23**, 861–867.
25 F. Bellezza, A. Cipiciani, L. Latterini, T. Posati and P. Sassi, *Langmuir*, 2009, **25**, 10918–10924.
26 S. Mandal and S. Mayadevi, *Chemosphere*, 2008, **72**, 995–998.
27 T. Hibino, *Chem. Mater.*, 2004, **16**, 5482–5488.
28 Q. Su, S. Pang, V. Alijani, C. Li, X. Feng and K. Müllen, *Adv. Mater.*, 2009, **21**, 3191–3195.
29 M. K. Stern, M. P. Jensen and K. Kramer, *J. Am. Chem. Soc.*, 1996, **118**, 8735–8736.
30 J.-H. Fuhrhop, *Langmuir*, 2014, **30**, 1–12.
31 F.-T. Zhang, X. Long, D.-W. Zhang, Y.-L. Sun, Y.-L. Zhou, Y.-R. Ma, L.-M. Qi and X.-X. Zhang, *Sens. Actuators, B*, 2014, **192**, 150–156.
32 L. Chen, N. Wu, B. Sun, H. Su and S. Ai, *Microchim. Acta*, 2013, **180**, 573–580.
33 A. Vandervliet, J. P. Eiserich, C. A. Oneill, B. Halliwell and C. E. Cross, *Arch. Biochem. Biophys.*, 1995, **319**, 341–349.
34 S. Vial, V. Prevot, F. Leroux and C. Forano, *Microporous Mesoporous Mater.*, 2008, **107**, 190–201.
35 E. Geraud, V. Prevot, C. Forano and C. Mousty, *Chem. Commun.*, 2008, 1554–1556.
36 C. Mousty, O. Kaftan, V. Prevot and C. Forano, *Sens. Actuators, B*, 2008, **133**, 442–448.
37 K. Charradi, C. Forano, V. Prevot, D. Madern, A. Ben Haj Amara and C. Mousty, *Langmuir*, 2010, **26**, 9997–10004.